

# Simulation of SARS-CoV-2 epidemic trends in Tokyo considering vaccinations, virus mutations, government policies and PCR tests

Jianing Chu, Hikaru Morikawa, Yu Chen\*

Department of Human and Engineered Environmental Studies, Graduate School of Frontier Science, The University of Tokyo, Kashiwa, Chiba, Japan.

**SUMMARY** The eighth wave of COVID-19 infection in the Tokyo area has brought daily confirmed cases to a new higher level. This paper aims to explain the previous seven epidemic waves and forecast the eighth epidemic trend of the area using agent-based modeling and extended SEIR denotation. Four key considerations are investigated in this research, that are: 1. Vaccination, 2. Virus mutations, 3. Government policies and 4. PCR tests. Our study finds that the confirmed cases in the previous seven epidemic waves were only the tip of the iceberg. Using data prior to December 1 2022, the eighth wave is expected to hover high in December 2022 and January 2023. Our research pioneers in the simulation of antibody titer declination on an individual level level. Comparing the simulated results, we find that the arrival of new epidemic waves are related to the decline in the number of antibody possessors, especially during the sixth and the seventh epidemic waves. Our simulation also suggests that faced with low severe and low death rates, PCR tests would not make much difference to reduce overall infections. In this case, maintaining PCR tests to a low level helps to reduce both social cost and public anxiety. However, if faced with the opposite case, PCR tests should be adjusted to a higher level to detect early infections. Such level of PCR tests should be compatible with available medical resources.

**Keywords** Agent-based modeling, COVID-19, Vaccination, IgG, PCR testing.

## 1. Introduction

On January 24, 2020, the Tokyo Metropolitan Government detected the first case of COVID-19 infection (1). After this detection, Japan promptly took various actions, including distributing masks to households and banning entries from 159 countries and regions. There have already been seven waves of infections since then until October 2022. The epidemic trends in Tokyo have different characteristics compared with those in New York, London and other European countries. Daily confirmed cases of the three cities (Tokyo, New York and London) reached a coincident historical high in January 2022. Daily infections have dropped since then for New York and London, while the reported cases in Tokyo continue to surge to a new high in August 2022. We notice that there is still no timely study on the reason behind such a difference in the past waves, In the meantime, no comprehensive study has been conducted to predict the epidemic trend for the eighth wave based on different scenarios. At the outset of research, we assume that four factors, namely vaccination rollouts, virus mutation, government policies and PCR tests mainly influenced the epidemic trend, under the following

considerations: 1) vaccination helps provide antibodies so as to reduce the Coronavirus spread; 2) viruses with mutations may become more infectious by escaping immunity; 3) the government can set up regulations regarding travel restrictions and *etc.* aiming to slow down the spreading of virus; and 4) the capacity of PCR tests has nontrivial impacts on the number of confirmed cases. The reasons for choosing the first three factors are relatively clear, while the reason to include the PCR tests needs a further explanation. In short, there exists a strong correlation between the number of conducted PCR tests and the number of confirmed cases, details of which shall be discussed in Sec. 1.4.

There has been existing research related to our study. Chiba (2) discusses the measures to control epidemic spread in Japan from three aspects: mobility control, reducing restaurant hours and working at home. Yamauchi and others (3) examine the association between epidemic dynamics, government measures and the daytime population in Tokyo. Murakami and others (4) use agent-based modeling and GPS analysis to simulate infection spread and inhibition in Tokyo, addressing the importance of city lockdown and prevention measures in service facilities. Yasuda and others (5) suggest vaccine

distribution strategies based on behavioral differences between residents in Tokyo and Osaka and conclude that high-risk older adults should be given priority when vaccine supplies are sufficient, but if vaccine supplies are scarce, vaccination of specific groups affected by the epidemic should be considered preferentially. It is worth noting that none of the above research took the vaccination, antibody titer declination, traveling policies, virus mutation, agents' heterogeneity and the advocacy of PCR testing all into account, while our study is partially motivated by such a research gap.

This research employs SEIR denotation (see Table 1) and agent-based model building. We shall discuss details in the methodology part. Actual data of the aforementioned four factors are provided by the Tokyo Metropolitan Government and shall be fed into our model for validation. We expect that simulations can not only explain the emergence of the past seven waves but also be able to forecast the future trend of coronavirus infections. Specifically, our research aims to reproduce the arrival, the rise and decay, as well as the maximum number of daily infections for each wave. Moreover, the parameters of the model are subject to continuous revision based on online data published by the Tokyo Metropolitan Government, so that we can make timely predictions about future pandemic trends by creating different scenarios. Last but not the least, we hope this research could help to make some recommendations to government policies that may mitigate or even prevent future waves of infection.

We organize the paper as follows: In the Introduction part (Sec. 1), we discuss the four key considerations and their significance to our research. In the Materials and Methods part (Sec. 2), agent-based modeling and extended SEIR modeling approaches are discussed. Also, a detailed explanation on the construction of our model is presented together with a cautious verification and calibration. Then, prudent predictions are put forward in Sec. 3 with six scenarios being considered. Lastly, we summarize our findings and recommendations in the conclusions part (Sec. 4).

We performed a prior investigation on the four postulated factors based on open-source public information and the Tokyo Metropolitan Government website (1). All the data and information collected here are used in the model building described in Sec. 2.2.

### 1.1. Vaccination

It is evident that mass vaccination helps to reduce severe rate and death rate (6). Table S1 (<http://www.biosciencetrends.com/action/getSupplementalData.php?ID=134>) summarizes the five rounds of vaccination that have been carried out in Tokyo. At the latest update, Tokyo began the rollout of bivalent shots targeting Omicron variant on September 20, 2022, restricted to those aged 60 and over, and those with preexisting medical conditions as well. Because over 90% of

**Table 1. Summary of eight health status of agents and their meanings**

States	Meanings
S1	Susceptible, Healthy, without antibody and vaccination record
E	Within the infection distance to I1 agents, potentially infected
I1	Infected, not unconfirmed and not tested
I2	Infected, confirmed through PCR test
V	Healthy, vaccinated and antibody carried
R	Healthy, cured and antibody carried
S2	Healthy, susceptible, vaccinated but antibody lost
D	Dead

Coronavirus deaths in Japan have been among those aged 60 and older, the rollouts aim to protect the vulnerable and reduce the overall death cases. We notice that Tokyo began the rollout of bivalent shots for all citizens in late October 2022, as the confirmed cases surged to a new high.

### 1.2. Virus mutations

Table S2 (<http://www.biosciencetrends.com/action/getSupplementalData.php?ID=134>) summarizes the dates when the notorious mutated viruses were first detected in Japan. Effective reproduction number and severe rate of these viruses are listed in the right columns of the table. As Table S2 (<http://www.biosciencetrends.com/action/getSupplementalData.php?ID=134>) shows, the current trend is that the virus is becoming more infectious periodically judging from the effective reproduction number while less lethal thanks to the combined efforts of continuously advanced policy measures, vaccinations and medical treatments.

### 1.3. Government policies

When considering government policies, this paper points to the city governance, guidelines for medical treatments, restrictions of border measures and prevention acts towards the Olympics *etc.* The Tokyo Metropolitan Government had imposed a total of seven announcements of emergency states, as shown in Table S3 (<http://www.biosciencetrends.com/action/getSupplementalData.php?ID=134>). Standard regulations were applied in four of these emergency states, and three relaxed regulations were applied in the remaining ones. Tokyo city also adopted the Highly Active Anti-Retroviral Therapy (HAART Therapy, *HAART Therapy comprises the use of two or more monoclonal antibodies, minimizing the risk of drug-resistant virus strains developing.*) for COVID-19 treatment from July 19, 2021, thanks to the proposal of Ms. Yuriko Koike, who was the metropolitan's first female governor. Referring to Table S4 (<http://www.biosciencetrends.com/action/getSupplementalData.php?ID=134>), the adoption of HAART Therapy had greatly decreased the overall death rate. On November 22, 2022, Ministry of Health, Labour and Welfare of Japan granted the emergency use of Shionogi's oral drug

'Xocova' for COVID-19 treatment of those aged over 12 (7). The distribution of 'Xocova' started on November 28, 2022, covering about 2,900 medical facilities and supplying 1 million citizens. It is believed that the severe rate and death rate can be further reduced in the near future.

As for the border measures, we summarize timelines of various regulations in Table S5 (<http://www.biosciencetrends.com/action/getSupplementalData.php?ID=134>). Japan had shortly opened its border to foreign residents twice in 2020. After March 1, 2022, the country allowed foreign nationals to enter into the country for non-tourism purposes. On June 10, 2022, Japan reopened its border and began to accept group tours from 98 countries and territories (8). The first tour group of tourists landed at Narita Airport on June 22, 2022 (9).

Japan held the Tokyo Olympics from July 23, 2021, until August 8, 2021. The country welcomed the first foreign Olympic team on June 1, 2021 (10). The International Olympic Committee (11) required athletes to depart no later than 48 hours after completing their competition, which implies that the period of leaving starts from July 25, 2021, and lasts until August 10, 2021. Approximately 79,000 people flew to Japan for the Tokyo Olympics (12). Details are summarized in Table S6 (<http://www.biosciencetrends.com/action/getSupplementalData.php?ID=134>).

#### 1.4. PCR tests

In Tokyo, PCR tests can be either conducted by the Tokyo Metropolitan Institute of Public Health or at medical institutions, with the latter one undertaking the major inspection work. In general, Tokyo citizens take PCR tests on a voluntary basis, following doctor's advice as well as their judgement of their own health condition, *i.e.*, symptoms of Coronavirus infection such as high fever, cough, headache, fatigue. The shortage of PCR capacity has been constantly criticized. As was reported on February 18, 2022, faced with the sixth wave of infection driven by Omicron variant, shortages of antigen and PCR kits are still commonplace (13), even two years past the initial outbreak.

The Japanese government has urged to boost PCR testing capacities as well as antigen productivity. According to the Ministry of Health, Labour and Welfare of Japan, PCR tests have been covered by medical insurance since March 6, 2022, which means that medical institutions can directly request tests from private testing institutes and other such bodies. Also, with the insurance coverage approval for antigen detection kit "Lumipulse SARS-CoV-2 Ag", saliva-based tests became available to asymptomatic patients from July 17, 2022 (14). In addition, residents can request a free antigen test kit delivered to their residence upon registration on the Tokyo Metropolitan Government website (15), if they deem themselves to have symptoms or become close

contacts. This act can ease the concentration of tests and consultations at medical institutions. If the antigen test result is positive, the testee can immediately start a 14-day self-quarantine to avoid further spread of the infection.

These measures together encourage the public to take tests as well as help to detect individuals with infectivity, as can be inferred in Figure 1A, where we sum up the number of PCR tests conducted on a daily basis (2020.01.24 ~ 2022.11.30). We also conduct a linear regression test between daily confirmed cases and daily numbers of PCR tests. The results show a multiple R-square value of 0.4843 and a  $p$ -value of  $2.2 \times 10^{-16}$ . Accordingly, we consider that there is a relatively strong correlation between the number of PCR tests and the number of confirmed cases. This explains why we consider the PCR testing capacity as a critical issue.

#### 1.5. Other considerations

School vacation is another factor considered in this research. We list the vacation periods in Table S7 (<http://www.biosciencetrends.com/action/getSupplementalData.php?ID=134>). During these vacations, students are apt to travel farther than they do in terms. Summer vacation in 2021 is an exception due to the scheduled 4<sup>th</sup> announcement of a state of emergency.

## 2. Materials and Methods

### 2.1. Methodology

#### 2.1.1. Agent-based modeling

In this study, we use NetLogo (16), a beautiful agent-based modeling tool (ABM), for simulation of the epidemic dynamics. The main reason lies in that agent-based modeling can help represent the fine-scale individual heterogeneity faced with complex environments. When describing a large-scale epidemic phenomenon, differences in individual attributes may not be neglected because of the strong social and physical interaction among people. Typically, people have different occupations and versatile behavior patterns, thus their response to the Coronavirus and the vaccination are diverse. At the aggregated level, these differences tend not to be averaged out, implying that modeling of heterogeneity is essentially necessary. In contrast, the major difficulty in applying ABM to the simulation of epidemics is the validation of the model with the real data. Although ABM can mimic the micro-level infection process among individuals, which is basically determined by human-to-human distance, the straightforward feeding of the reported  $R_0$  coefficients into the model is not feasible. Nevertheless, ABM can be calibrated by tuning the model parameters so that the calculated  $R_0$  of the model may agree with that measured in the real world.

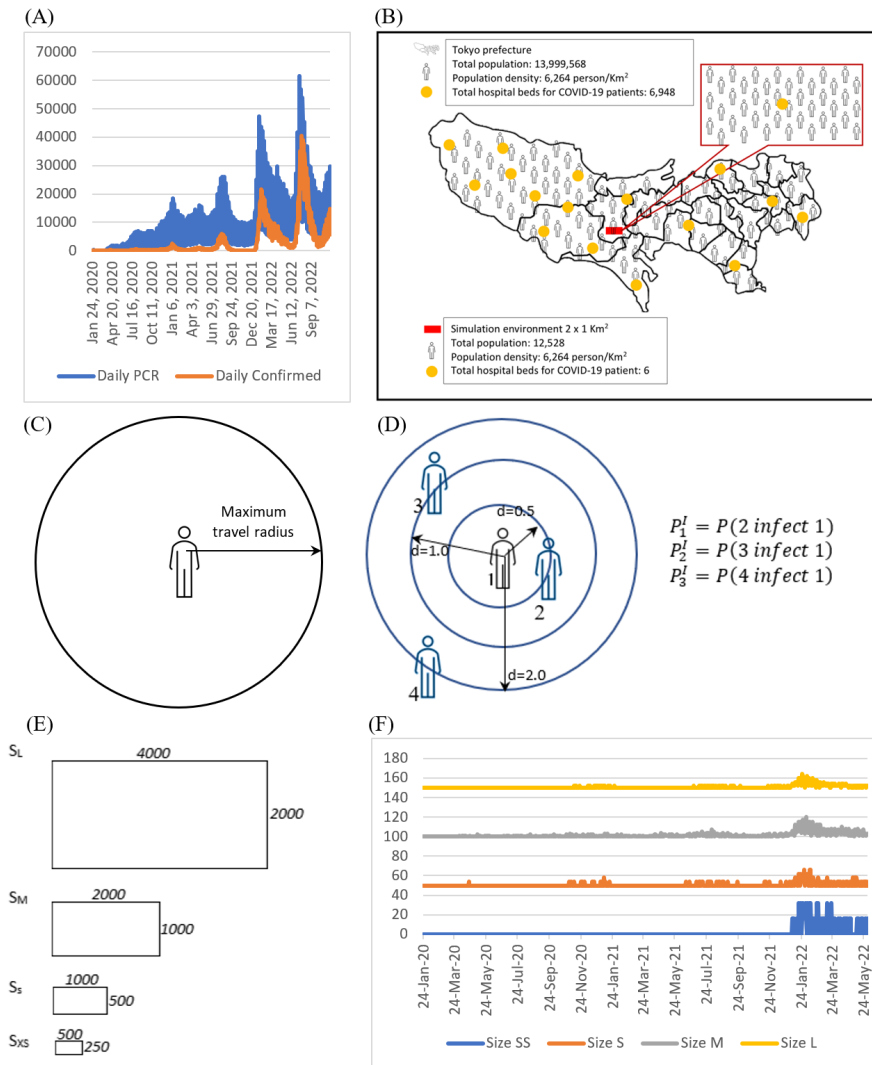


**Figure 1. PCR test and confirmed cases; scaled simulation environment, moving patterns and validation of down-scaling.** (A), The number of daily conducted PCR tests and daily confirmed cases from 2020.01.24 to 2022.11.30. (B), Illustration of the simulation environment after scaling down. (C), Illustration of agents' moving pattern (see Appendix 3). (D), Illustration of agents' infection pattern (see Appendix 2). (E), Models with different patch sizes. (F), Simulation of models with different sizes.

We are aware that numerous ABM studies on the epidemic dynamics have been done. Here we list some of the latest publications and specify the pros and cons of these models. A data-driven agent-based modeling framework (17) is designed to forecast Ebola trends, which comprises three parts: synthetic population, social contact network and disease model. The model not only has a good representation of work or school activities and long-range mobility but also performs well in forecasting. Shamil and others (18) use agent-based modeling to explore the impact of contact tracking and find the parameters that lead to termination of the epidemic in a city, though their research does not take vaccination into account. Li and Giabbanelli (19) study the effectiveness of vaccine campaigns, the willingness of being vaccinated and the vaccine capacity under different federal plans, with the interactions between nonpharmaceutical interventions and vaccines considered. Although their research

covers vaccines, it is noticed that vaccine efficacy decreases as antibody titers in the human body drop, let alone the virus mutates constantly. Kerr and others (20) develop the Covasim model to evaluate the effect of different interventions on the epidemic, including physical interventions, diagnostic interventions, and pharmaceutical interventions. Covasim, however, ignores influences from virus mutations, immigration policies and agents' heterogeneity. Comparing these researches, our study tries to take the effect of 4-dose vaccination, antibody titer declination, virus mutation, government policies, and PCR tests together into account.

### 2.1.2. Extended SEIR modeling

Our model denotes the health status of individuals by borrowing the idea of the SEIR model (Hethcote, 2000). However, we do not simply employ the standard

'Susceptible', 'Exposed', 'Infectious' and 'Recovered' status in the modeling. Because the SEIR model does not have 'vaccinated' or 'dead' status in its concept, it makes it not suitable for COVID-19 infection and vaccination studies. To overcome this deficiency of SEIR, we add the 'Vaccinated' and 'Dead' status and increase the resolution of description of the health status in the meantime, see the details in the model building part (Sec. 2.2).

We should supplement one more reason for the extension of the SEIR model. Although the traditional differential-equation-based SEIR model may conveniently take the measured  $R_0$  as an input parameter, the approach suffers from the so-called "time-lag effect," which means that we cannot accurately calculate the  $R_0$  coefficient without a large enough number of reported cases, while accumulating such a large sample takes time and resources. Especially when we face the continuous mutations of Coronaviruses, the fast variation of the reported  $R_0$  will cause the time-lag effect to be more severe. For example, a research team from Lancaster University came up with an  $R_0$  value of 3.8 in the original forecast version, then they updated the number to 2.5, considering many uncertainties, and before long they changed the number to 3.11 (21). Yang and others (22) also point out the flaws of using the SIR/SEIR model to estimate the basic reproduction number. In view of COVID-19's natural history, severe patients were often hospitalized, hence they should not be treated as transmitters. According to Yang's study (22), the  $R_0$  value used in SIR/SEIR calculations is usually underestimated.

In the ABM description of the epidemics, however, the infection process at the microscopic (human-to-human) level is much easier to be observed and measured, thus the reported condition for the infection will not change drastically along with the mutation of the virus. For example, a study (23) suggests that maintaining a social distance of 2 meters significantly reduces airborne dispersion of tiny droplets, hence the transmission risks from droplet inhalation. It takes approximately 7 seconds for viruses to be projected over a distance of 2 meters. Fundamentally, Coronavirus mutations have not changed such a microscopic mechanism of transmission.

Last, the original SEIR model cannot differentiate individuals by their occupations, work styles, moving patterns, *etc.*, hence the influence of heterogeneity at the small scales cannot be investigated easily. With an ABM, diverse attributes of the individuals can be naturally described by associating corresponding state variables and their updating algorithms to the agents.

## 2.2. Model

### 2.2.1. Space and population

A total of 13,999,568 people live in Tokyo city, which results in a population density of 6,264 persons per square

kilometer (24). The total number of hospital beds in the city is approximately 7,291 (1). Based on the assumption that all static properties (such as infrastructure) within Tokyo city are uniformly distributed, as well as that all dynamic properties (such as moving population) within the city are identical, our strategy is to build a rectangular block of 2 kilometers, which is geometrically similar to the Tokyo area, and simulate epidemic dynamics within this block using downscaled population and amount of infrastructure. See Figure 1B for more details.

By assuming the uniformity stated above, we linearly scale down the whole Tokyo region, which is composed of 23 municipalities, into a rectangular block with a length of 2km and a width of 1km. The synthetic population in the block is initialized at 12,528 and hospital beds at 6 in the block. We set the size of a patch as one square meter, so that totally  $2,000 \times 1,000$  patches are used to represent such a block. It is important to note that the population density and hospital density in Figure 1B are equal to the actual data. Based on government policies and the outbound and inbound statistics (see Appendix 1), the scaled number of entries and exits into and out of a block varies at each time step. Section 2.3.1 will examine the validity of this linear scaling.

We categorize 62%<sup>#1)</sup> (25) of the synthetic population as employees who engage in economic activities and let them have an above average mobility. We also categorize 17%<sup>#2)</sup> (26) of the population as students who attend school and have vacations in winter, spring and summer, as mentioned in Sec. 1.5. The other 21% are categorized as unemployed.

Regarding the vaccinated population, the 1<sup>st</sup>, 2<sup>nd</sup> and 3<sup>rd</sup> doses of daily vaccination number are collected from the website of the Tokyo Metropolitan Government (1). We assume the pattern of 4<sup>th</sup> dose daily vaccination to be the same as the 3<sup>rd</sup> dose. The daily data for the population who received the PCR test and who came, or left Tokyo are collected from the same website. All these daily numbers will be multiplied by the scaling parameter before being fed into the model.

### 2.2.2. Social contact

We noticed that there are finer ways to model the microscopic behavior of agents and the interactions among them. For example, Venkatramanan and others (17) acquire data of daily activity patterns to simulate the flow of population. Specifically, they build the people-location network which allows them to assign agents to locations with durations of visit thus determining their contacts and interactions. As

<sup>#1)</sup> According to the Statistics Bureau of Japan, the work force participation rate in Japan from 2020 to 2022 is around 61% [61.5, 63%].

<sup>#2)</sup> According to the MEXT Japan, the total number of students enrolled in educational institutions in Tokyo is 2,348,260, composing approximately 17% of the total 13,920,000 population.

another example, Kerr and others (20) design the contact network with multiple layers in the Covasim model. The Covasim model was constructed with considerations of age structure and household size, using published data from UN Population Division 2019. They presume individuals to move between household, school, workplace and community contact layers during the day, with different probabilities of infection based on unique connections and connection weights. The two studies attempt to simulate the microscopic movements of agents as faithfully as possible. When designing our model, however, we adopted a strategy to largely simplify the social contact process thanks to the restrictions in computation time and workload. Methodologically, our approach can be defended by Kadanoff's theory on Lattice Gas Automata (27), which says that while building a microscopic model by minimally extract the essential properties of components, we can still get the desired macroscopic behavior of a system.

In our model, agents are randomly distributed initially, with their position being recorded as their residence. As shown in Figure 1C, we assume that at the beginning of a day, all agents, except for those quarantined ones, can walk outside randomly for 8 hours per day in any direction but within a radius  $r_{max}$ , a range which corresponds to their scope of daily

activities and depends on their social status (either employee, student or unemployed), see Appendix 1 for detailed numerical values. During the random walk, agents have a chance to meet other walking agents, so as to be infected or to infect others. When a day ends, agents shall move back to their designated residence.

Although the social contact model described in this paper may not fully describe interactions among individuals from a microscopic perspective, we expect its aggregated outcomes will not differ significantly from those observed in macroscopic epidemics. Indeed, our model performed well in mimicking the past waves of infection (see Figure 2A). A similar phenomenon was observed in the microscopic modeling of fluid flows: Although molecules and interacting potentials of different types of fluids differ, large-scale flow dynamics are governed by the same equation. Just as Wolfram stated in his book on complex systems (28), (that even though the underlying rules of different systems vary, the overall results are the same.

### 2.2.3. Detailed model building

The construction and the implementation of our model consists of three parts: the definition of agent states (Sec. 2.2.3.1), the specification of processes for the state transition (Secs. 2.3.3.2-2.2.3.7), and the design of code

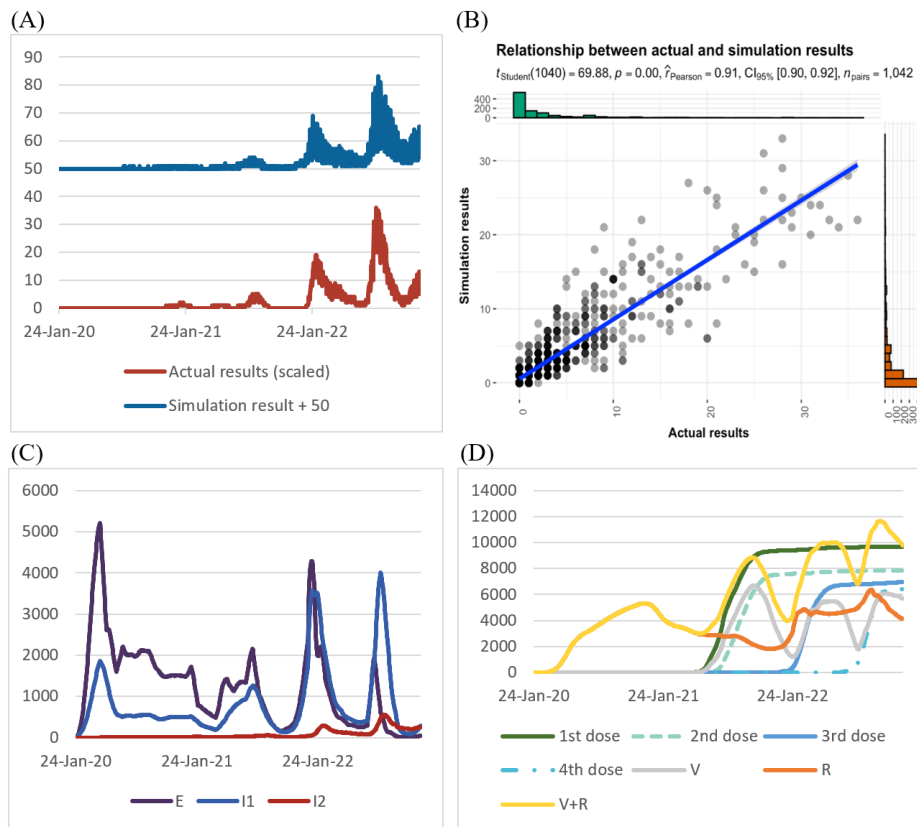


**Figure 2. Scaled actual results vs. simulation results, Infection, and vaccination.** (A), Actual results (scaled) vs. Simulation results from 2020.01.24 to 2022.11.30. (B), 'ggstatsplot' of simulation results and actual results. (C), The number of agents in E, I1 and I2 states from 2020.01.24 to 2022.11.30. (D), 1st, 2nd, 3rd and 4th doses of vaccination; the number of agents in V, R, V+R states from 2020.01.24 to 2022.11.30.

structure, which shall be presented in Appendix 2.

### 2.2.3.1. Health states and population

We extend the SEIR categorization to define totally eight health states for agents. This extension is necessary because it allows us to analyze the effect of vaccination on one side, while fully reflecting the pathological characteristics of COVID-19 on the other side. A summary of the available health states can be found in Table 1. Aside from the conventional S/E/I/R states, we have added the V state to represent the vaccinated individual who carries antibodies against Coronavirus. Furthermore, we separated the susceptible state into S1 and S2 in order to facilitate the modeling of booster doses based on those susceptible agents with antibody records (S2) and those without (S1). Additionally, we divide the infected state into two categories, I1 and I2. Since the confirmed cases (I2) will remain at home and self-quarantine once identified, they will lose their public infectivity in comparison with those infected but unconfirmed agents (I1). Additionally, we added the death state D.

There are a total  $N^{total}$  agents in the synthetic population. Among these agents, populations in different states are denoted as  $N^{S1}$ ,  $N^{S2}$ ,  $N^E$ ,  $N^{I1}$ ,  $N^{I2}$ ,  $N^V$ ,  $N^R$ ,  $N^D$ , respectively.

### 2.2.3.2. Susceptible

At  $t = 0$ , all agents are initialized to be in the Susceptible state (S1), with no one infected with Coronavirus. Home positions are recorded for agents, and they can move from home to places within a radius  $r_{max}$  (whose numerical values are listed in Appendix 3). Outing of agents lasts eight hours a day, regardless of direction. Once the space boundary is touched, the agent shall bounce back.

### 2.2.3.3. Exposure

As the imported cases begin to spread over the Tokyo region since January 24, 2020, we set this date  $t = 1$ . Over time, susceptible agents, if exposed to the asymptomatic cases (I1 agents), will have a likelihood to be infected. The odds for a state change from Susceptible to Exposed (S1→E) reads as the following

$$P_{S1 \rightarrow E} = H(d_{S1,I1} - d_E) \quad (1).$$

where  $H(x)$  is the heaviside step function, and  $d_{X,Y}$  stands for the shortest distance in the space between agents in state X and agents in state Y. The threshold distance  $d_E$  is set to 2 units of patch size, based on the statistics made by the Ministry of Health, Labour and Welfare (MHLW), saying that a physical distance within 2 meters can be deemed as close contact with Coronavirus transmission

possibility (29).

### 2.2.3.4. Infection

The probability for an exposed agent (in state E) to be infected by Coronavirus depends specifically on the distance when the agent met an agent in state I1, see Figure 1D.

The probability of infection ( $P_{E \rightarrow I1}$ ) is defined differently in three cases,

$$P_{E \rightarrow I1} = \begin{cases} P_1^I & 0 \leq d_{S1,I1} \leq 0.5 \\ P_2^I & 0.5 < d_{S1,I1} \leq 1.0 \\ P_3^I & 1.0 < d_{S1,I1} \leq 2.0 \end{cases} \quad (2).$$

Here values of  $P_1^I$ ,  $P_2^I$  and  $P_3^I$  are specified in Table S8 (<http://www.biosciencetrends.com/action/getSupplementalData.php?ID=134>). Each time the virus mutates, probabilities of infection will be adjusted according to the properties of viruses. If luckily the exposed agents are not infected, their states will change back to S1 (E→S1) by the following probability

$$P_{E \rightarrow S1} = 1 - P_{E \rightarrow I1} \quad (3).$$

All agents, except those who have been confirmed to be infected (in state I2), will receive PCR tests with a probability ( $P^T = \frac{n_T}{N^{total} - N^{I2} - N^D}$ ) per day, where  $n_T$  is the down-scaled daily number of PCR tests published by the Tokyo Metropolitan Government. As soon as the infectivity is confirmed by the PCR tests, the I1 state of infected agents will be re-marked as I2 state, implying that the transition probability can be calculated for an individual as the following,

$$P_{I1 \rightarrow I2} = \frac{P^T}{N^{total} - N^{I2} - N^D} \quad (4).$$

If currently an agent is in state I2, it will not be allowed to move anywhere until the next state transition either to R (recovery) or to D (death).

### 2.2.3.5. Recovery or death

Part of the confirmed patients (agents in I2) are transferred into hospital if there are available beds, in this way patients who receive medical treatment will have a lower death rate than those who are in self isolation. In the model, a local hospital is set up in the simulation space to model the treatment of confirmed patients with severe symptoms. The number of acceptable patients for the hospital is determined by referencing to the Tokyo Metropolitan Government website (1), which provides a list of the total capacity of hospital beds for COVID-19 patients. The capacity of the hospital is updated every day if recovered patients (agents in R) are discharged and newly confirmed patients (agents in I2) are admitted.

For agents in hospitals, the recovery (I2→R) rate is assumed to be 100%, whereas the fatality rate  $P^F$

outside of hospitals is determined by the therapies for Coronavirus treatment (See Table S4, <http://www.biosciencetrends.com/action/getSupplementalData.php?ID=134>). Confirmed agents (I2), if not transferred to hospital (self-quarantined), will become either self-cured (I2→R) or dead (I2→D) after fourteen days with the following probabilities,

$$P_{I2 \rightarrow R} = 1 - P^F, P_{I2 \rightarrow D} = P^F \quad (5).$$

If the infected agents are not confirmed by PCR tests within fourteen days after infection, they may move freely in the simulated block until self-cure (I1→R) or death occurs (I1→D) with the following probabilities

$$P_{I1 \rightarrow R} = 1 - P^F, P_{I1 \rightarrow D} = P^F \quad (6).$$

### 2.2.3.6. Vaccination

All surviving agents except confirmed ones (I2) are eligible to receive vaccination as long as there are remaining quotas. The health state of the vaccinated changes after a dose of vaccination (S1/E/I1/R/V/S2→V). Between the first and second dose, the duration is 5 to 8 weeks, between the second and third dose is 6 months, and between the third and fourth dose is 5 months.

Although the standards of efficacy testing vary, we can make an approximate estimation of Pfizer's vaccines' efficacy based on published clinical reports. A Pfizer vaccine has a first dose efficacy of 52% and a second dose efficacy of 91% (30). Although Tokyo residents can choose between different brands of vaccines, we model vaccine efficacy based on Pfizer's data. In particular, we take into account the decay of antibody titer, which has not been considered in other literature to the best of our knowledge.

For each vaccinated agent in the model, the probability of successfully obtaining the antibody *via* the first dose reads as the following

$$P_{S1/E/I1/R \rightarrow V} = \frac{n_V}{N^{S1} + N^E + N^{I1} + N^R} \times 52\% \quad (7).$$

Here the down-scaled daily vaccination quota  $n_V$  can be obtained from the record of the Tokyo Metropolitan Government. Similarly, the probability of successfully obtaining the antibody *via* the second, third, or fourth dose vaccination is

$$P_{S1/E/I1/R/V/S2 \rightarrow V} = \frac{n_V}{N^{S1} + N^E + N^{I1} + N^R + N^V + N^{S2}} \times 91\% \quad (8).$$

Additionally, we consider that there may be an extremely small possibility that agents may die after each vaccination (V→D)

$$P_{V \rightarrow D} = 8.1 \times 10^{-6} \quad (9).$$

Numerical value of this death rate is given by the study

by Yamaguchi and others (31), which indicates that 1,315 cases over 163,059,502 doses of Pfizer vaccination became dead in Japan as of October 15, 2021.

### 2.2.3.7. Antibody titer declination

Antibodies are acquired through vaccination or self-cure. It is commonly observed that self-recovered people have slower antibody titer decline rates than vaccinated ones (32). The immunoglobulin G (IgG) test is a commonly performed method for determining COVID-19 antibody titer levels. Narasimhan *et al.* (33) identified anti-SARS-CoV-2 IgG-positive immune responses after vaccination based on a positive threshold of 50 AU/mL. Ebinger and others (34) proposed that 4160 AU/mL (corresponding to an ID50 of 1:250) could be used as a surrogate marker of serum neutralizing activity.

In our model, antibody titer levels (IgG levels) for each agent decrease over time as determined by linear regression of data from previous studies. Once agents' antibody titer levels drop below a threshold, which is determined by calibrating the model with actual data in Sec.2.3.2.3, their status will change to S2 (V/R→S2).

According to Ariel Israel and others (32), individuals who received Pfizer-BioNTech's mRNA vaccine have differing antibody titer levels when compared with patients who were infected with the SARS-CoV-2 virus. As a result, antibody concentrations acquired from vaccination are higher initially, but decrease exponentially at a much faster rate (32). Based on their research, the antibody titer  $Y(t)$  measured in AU/mL after SARS-CoV-2 infection may be expressed as  $Y(t) = 357 \times 0.96^{t'}$ , where  $t'$  is 'month (s)' since the positive PCR tests. Converting into the daily antibody titer change for the self-recovered agents (I1/I2→R), we use the following formula for our model

$$Y(t) = 357 \times 0.998640^{(t-t_i)} \quad (10).$$

where  $t-t_i$  represents day(s) since the time of infection ( $t_i$ ). The change of IgG after the first/second/third/fourth doses have been done in another study (35). Data are listed in Table S9 (<http://www.biosciencetrends.com/action/getSupplementalData.php?ID=134>).

Despite the scarcity of data, we may assume the decay of antibody titer acquired from the vaccination follows the power law function found in the decay of antibody titer in the naturally immune case. We simply apply linear regression to the logarithmic coordinates

$$\log D = \frac{1}{t_2 - t_1} [\log Y(t_2) - \log Y(t_1)] \quad (11).$$

where  $D$  is decay rate of antibody titer,  $t_1, t_2$  are two separate timing measurements after the vaccination. As a result, we obtained the following formula for the decay of antibody titer acquired from vaccination of different doses

$$Y(t) = Y_0 \times D^{(t-t_0)} \quad (12).$$

where  $Y_0$  is the initial antibody titer after a specific dose of vaccination,  $D$  is the decay rate of antibody titer with respect to the elapsed time measured in day(s) since the vaccination, and  $t_0$  the time of vaccination. Numerical values for these parameters in different doses of vaccination are summarized in Table S10 (<http://www.biosciencetrends.com/action/getSupplementalData.php?ID=134>).

In practice, as we understand that as COVID-19 virus keeps mutating, vaccines are becoming less protective, we set a relatively fast declination rate as  $D = 0.980916$  in our simulation code for all four doses of vaccination. This simplification is in accordance with the study by Xu *et al.* (36), in which authors found that the concentrations of antibodies will increase rapidly after receiving the second dose vaccine and will reach their peak around two weeks (14 days) following the second dose vaccination. Typically, the peak will last for one week and then begin to decrease after three weeks (21 days).

### 2.3. Verification and Calibration

#### 2.3.1. Verification of linear scaling

In Section 2.2.1, we linearly scale down the entire Tokyo region into a rectangular block with a length of 2km and a width of 1km, containing 12,528 susceptible agents and a hospital that can accommodate 6 infected agents. However, there is still the question of whether, after the simulation has been completed, the results can be scaled back to Tokyo in the real scale. To prove this scaling relationship, we first assume that the confirmed infected population in the real world depends on the area and the total population as the following

$$N^{I2}(S, N^{total}; t). \quad (13)$$

Now if we use a parameter  $\lambda < 1$  and perform a simulation in the down-scaled area  $\lambda S$  and population  $\lambda N^{total}$ , can we obtain the infected population  $N^{I2}$  in real space by simply scaling up the simulation results by a factor of  $1/\lambda$ ? The answer is that if the following relation holds true

$$N^{I2}(\lambda S, \lambda N^{total}; t) = \lambda N^{I2}(S, N^{total}; t) \quad (14)$$

results in the original scale can be obtained by linear scaling of the simulation results.

To justify this argument, let us set  $\lambda = 1/4$  and perform the simulation on four areas  $S_L, S_M, S_S$  and  $S_{XS}$ , as shown in Figure 1E. Note that we have  $S_L:S_M:S_S:S_{XS} = 4:1:(1/4):(1/16)$ , in the meantime, we adjust all quantities including number of agents, hospital, entry and exit, daily vaccination and PCR test rates according to this ratio, but keep the maximum travel distance  $r_{max}$  fixed. If linear scaling applies in this extended SEIR modeling, our expectation is that we may have the following

relation

$$N_L^{I2}/4 = N_M^{I2} = 4N_S^{I2} = 16N_{XS}^{I2} \quad (15)$$

where  $N_Y^{I2}$  is the population of confirmed infection obtained from a simulation in the scaled area  $Y$ . In the validation, we set  $S_M$  the same size as the model in our study, representing the  $2km^2$  block by  $2,000 \times 1,000$  patches, while other scaled areas are set as  $S_L = 8km^2$ ,  $S_S = 0.5km^2$ , and  $S_{XS} = 0.125km^2$ . After we obtain the daily infection data from simulations in blocks with different sizes, we show the scaled number of daily infections in Figure 1F, where data are differentiated by shifting with a constant for visualization.

Inspecting results obtained from simulations with different areas may reveal that the scaled dynamics are essentially the same, however time resolution is limited by the size of the simulation block. Moreover, we also find that the shape of the simulation area does not matter, as the scaling relationship merely depends on the area and population. As a result of this validation, we are confident to use the current model to perform the simulation in a small rectangular block to examine, after scaling up the results, the trend of infection in the real Tokyo area, under the assumption that distributions of everything in Tokyo are uniform.

#### 2.3.2. Calibration of the model

In order to calibrate the model, we use data on the confirmed infection cases from January 24, 2020, to October 1, 2022. Parameters such as hospital capacity, initial population, *etc.*, are set in the initialization module of the code, while parameters under adjustment are antibody thresholds and infection probabilities in social contact of the agents.

##### 2.3.2.1. Fixed parameters

The parameters that are given at the beginning and fixed during the simulation are summarized in Table S11 (<http://www.biosciencetrends.com/action/getSupplementalData.php?ID=134>). The reasons or backgrounds for such parameter settings are described in Sec. 1 through Sec. 2.2.

##### 2.3.2.2. Parameter adjustments

Recall that we consider four key factors in Sec. 1 that have impacts on the epidemic trends, namely the vaccination, the mutation of virus, the traveling policies and the PCR tests. To reproduce the daily infected cases that correspond with those of the actual data, we select two model parameters, namely the threshold concentration of antibodies and the probability of infection over different contacting distances between agents in state II and others, as the parameters to

be adjusted manually. The reason for this choice is explained as follows.

In the calibration of the model, quantities related to traveling policy and PCR tests are not to be adjusted, since there is actual data recording the inbound/outbound populations as well as PCR tests performed in the Tokyo area. We simply take these data as input to the simulation. On the other hand, although the daily numbers of vaccination have also been given, the decay of antibodies of each vaccinated person is not known. This uncertainty in the cutoff concentration of antibodies can be utilized to tune the simulation results. Regarding the mutations of the Coronaviruses, they will result in a different probability of infection. Even though we know the change in the infectivity due to the mutation, we may not be able to measure this probability under various circumstances accurately. This fact provides another space for the adjustment of model parameters.

As a result of trial and error, we found that the cutoff or threshold for antibody effectiveness should be set at 250 AU/mL, below which agents would lose antibodies and be susceptible again. We tested this threshold several times and found this value leads to simulations that are most closely related to Tokyo's case numbers. In fact, the antibody response is heterogeneous (influenced by age, gender, comorbidities, genetics, and other inter-individual variations), for simplicity, we still use 250 AU/mL as a universal cutoff point.

Results of adjusting the probability of infection are shown Table S8 (<http://www.biosciencetrends.com/action/getSupplementalData.php?ID=134>). For variants of the same class, we let  $P_1^I$  to remain the same, while increasing  $P_2^I$  and  $P_3^I$  by 5% or 10% at a time. For instance, Compared With the original Delta variant, Delta N501S is assumed to have the same  $P_1^I$  as the original Delta, however, but 5% higher in  $P_2^I$ . Similarly, compared with the original Omicron variant, Omicron BA.2 is assumed to have the same  $P_1^I$  as other Omicron variants, yet 5% higher in its  $P_2^I$  and  $P_3^I$ . Nevertheless, the new arrival of Omicron variants XE and BA.2.75 are considered as exceptions due to their high immunity escaping abilities.

### 2.3.2.3. Reproducing the seven waves

By adjusting model parameters above, our goal is to reproduce in the simulation, the past seven waves of infection that have been reported in the Tokyo area. Details of these waves of infection are described below..

Table S12 (<http://www.biosciencetrends.com/action/getSupplementalData.php?ID=134>) summarizes the dates and the maximum daily confirmed cases in the past epidemic waves in Tokyo. Immediately following the outbreak of the first wave in late March 2020, Japan implemented PCR testing criteria, closed schools, promoted teleworking, and encouraged people to wear masks. The implementation of the first state

of emergency resulted in a 68% reduction in subway passengers, which controlled the infection effectively. After the state of emergency, the second wave began and subsided without further state of emergency measures, a phenomenon that can be explained by the increase in PCR testing capacity (37). The second emergency state was declared during the third wave of infection, local governments called for a reduction in business hours and restrictions on activities. With the spread of Delta variant, the advantage of public vaccination became evident in the fourth wave of infection. In contrast to 2,520 cases per day in the third wave, the maximum number of confirmed cases per day was controlled below 1,126. Along with the opening of the Tokyo Olympic Games and the spread of mutated Delta virus, the fifth wave arrived. Despite the declaration of emergency and the first-dose vaccination, the maximum daily confirmed cases reached 5,908. A surge in the confirmed cases in the sixth wave of infection occurred following the outbreak of Omicron variant in late December 2021. The seventh wave of cases started in mid June 2022, dominated by the BA.5 subvariant. Variants Omicron BA.2, Omicron XE, Omicron BA.4 and BA.5 brought the number of newly confirmed cases to a higher level. There were no further emergency measures taken by the Tokyo Metropolitan Government. On the contrary, reopening policies have been implemented to accept groups of tourists from outside Japan. The number of maximum daily infections reached 40,395 on July 28, 2022, almost twice as many as in the sixth wave.

Figure 2A shows the comparison of scaled actual data versus the simulated COVID-19 daily infection cases in Tokyo from 2020.01.24 to 2022.11.30. We obtain the simulation results by averaging the data after 60 times of calculations. Compared with the scaled infection data, we note that our model has successfully reproduced the well-known seven waves of infections in the Tokyo area. Moreover, our model can also correctly predict the maximum daily confirmed infections in each wave, see Table S13 (<http://www.biosciencetrends.com/action/getSupplementalData.php?ID=134>).

Figure 2B shows the scatter plot combined with marginal density plus histogram. These results are obtained by using 'ggscatterstats' in the package 'ggstatsplot' (38). The number of data  $n_{pairs} = 1042$  corresponds to the period 2020.01.24 ~ 2022.11.30. As can be seen from the graph, we use  $p = 0.00 < 0.05$  to reject the null hypothesis. The statistical significance between two groups is supported by  $r_{Pearson}^2 = 0.91$ , which lies in  $CI_{95\%}[0.90, 0.92]$ . Overall, the statistical analysis shows that simulation results agree with the actual data well. We also performed granger causality tests on the two groups of results. The granger causality test is a common practice used to examine if one time series may be used to forecast another. After the calculation, the  $F$  test statistic is equal to 64.008 and the p-value that corresponds to the  $F$  test statistic is  $Pr_{(>F)} = 2.2 \times$

$10^{-16} < 0.05$ . Thus, we may reject the null hypothesis and conclude that our simulation results are useful for predicting the actual results.

### 2.3.3. Findings

#### 2.3.3.1. The unconfirmed infected cases

From Figure 2C, we can see the number of agents in E, I1 and I2 states from January 24, 2020, to November 30, 2022, with their lines marked in purple, blue and red respectively. Figure 2D shows the simulated 1st, 2nd, 3rd and 4th doses of vaccination from January 24, 2020, to November 30, 2022. Figure 2D also shows the number of agents in V, R and V+R states from January 24, 2020, to November 30, 2022. From the observation, we find the following phenomena.

1. As the I1 population increases, the E population surges, which confirms the observation of a positive loop of infection, which implies that the more infected agents, the more exposed agents, and the wider the spread of infections.

2. Since Coronavirus mutations cause an increasing trend of infection probabilities, the difference between populations E and I1 gradually narrows until the late 6th wave. Since the announcement of the reopening policies for non-tourism purposes on June 1, 2022, it is assumed that asymptomatic carriers overseas rush into Japan, causing a rapid increase in I1. Nevertheless, due to the strong protective effect of the 4th dose vaccination starting May 25, 2022 (see Figure 2D), there were fewer E than expected, thus the gap between E and I1 started to broaden.

3. The PCR test numbers were low during the first to fifth epidemic waves, leading to low levels of daily confirmed infections. However, the actual numbers of agents in E and I1 states were high, suggesting that reported cases did not reflect real epidemic trends.

4. Due to the increase in PCR testing capacity, even though the number of E and I1 agents had dropped to historical lows post the 7th wave, the number of reported cases exceeded those during the previous waves.

In light of the strong correlation between PCR tests and daily confirmed cases, it is evident that the number of daily confirmed cases does not fully reflect the actual infection trends in Tokyo. In reality, the confirmed cases detected were only the tip of the iceberg.

#### 2.3.3.2. The reasons behind the seven waves

We hereby summarize the characteristics of the infection trends in Tokyo in Table S14 (<http://www.biosciencetrends.com/action/getSupplementalData.php?ID=134>). Below is a list of the reasons for bringing about these characteristics.

1. First, compared with New York and London,

Tokyo started its 1st dose vaccination not until the start of the 4th epidemic wave, which is deemed relatively late and vulnerable to future mutated viruses (Tokyo: April 12, 2021; New York: December 14, 2020; London December 8, 2020).

2. Second, the PCR testing capacity was comparatively low and could not reflect the real infection trends, especially during epidemic waves 1~5. (See Table S14, <http://www.biosciencetrends.com/action/getSupplementalData.php?ID=134>).

3. Third, the PCR testing capacity has improved since the 6th epidemic wave dominated by Omicron Oariant. It is believed by Larrauri and others that previous vaccination as well as self-cure together reduced the overall severe rate and death rate (6). However, the outdated antibodies (antibodies not targeting Omicron variant) cannot stop the mass spread of Omicron and its mutated variants. Therefore, the reported confirmed cases during the 6th wave were at an historical high.

4. Fourth, in accordance with the latest research (39), BA.2.75 can evade nearly all antibodies, no matter acquired from previous vaccination or self-cure. Even though the vaccination rates were at high levels in the 7th epidemic wave (see Figure 2D), mass spread seems inevitable. In this case, increased PCR testing capacity only leads to a higher level of daily confirmed cases, but limited effectiveness to control overall infection trends in the 7th epidemic wave.

## 3. Results

### 3.1. Scenario design

When designing different scenarios to forecast the future epidemic waves, we consider the two most important factors to be the number of daily PCR tests and the number of inbound/outbound travelers, the latter of which is the consequence of travel and border measures of the Japanese government. The other two factors, namely the vaccination rates and virus mutation are set in reference to actual data up to the end of November 2022.

The reason for choosing the number of PCR tests as one of the control parameters is that the number of PCR tests performed is not solely determined by the capacity provided by the government. Voluntary testing, the rate of which is influenced by decision making of each agent based on the published number of confirmed cases, will result in a positive feedback loop between the two dynamics. On the other hand, PCR tests can help to stop the spread of infection by screening out infectious agents by making them self-isolated. For these reasons, the pattern of PCR test number is considered unpredictable, thus needing to be discussed through the designed scenarios.

The numbers of in/outbound travelers are chosen as one of the key considerations because Japan has fully opened its border to oversea visitors since October 11,

2022, together with plans to revive its economy through the weakened Yen and the advertised tourism. Moreover, as winter holidays approach (Christmas, New Year, Spring Festival and *etc.*), it is likely that some citizens might consider going abroad for their holidays, which increases the risk of bringing the virus into Japan. Since the complexity in the real world makes these numbers difficult to be modeled, therefore they should be considered by postulated scenarios.

In contrast, the main reason for us not to choose virus mutations is that, under the premise of an increasing level of antibody obtained either from the infection of the Omicron variant or from the vaccination, probability of infection to the exposed is expected to have reached its limit. If a new variant emerges with stronger ability to escape immunity, we are more inclined to consider it a completely new virus rather than COVID-19. Lastly, by the end of November 2022, the third-dose vaccination rate has reached 65.7% among all Tokyo citizens and the fourth-dose vaccination rate has reached 80.4% among the elderly. Looking into the 1st, 2nd and 3rd doses of public vaccination, we find that the pattern of the vaccination trends does not differ much (1). As long as the government maintains its current plan to vaccinate the public, the vaccination trend of the 4th dose is expected to follow the previous ones'.

### 3.1.1. Parameter settings

We use past vaccination data as reference to generate the vaccination quotas from 2022.10.01 to 2023.02.01. As shown in the upper panel of Table S15 (<http://www.biosciencetrends.com/action/getSupplementalData.php?ID=134>), the 1<sup>st</sup>, 2<sup>nd</sup> and 3<sup>rd</sup> doses of vaccination records during November 13 ~ 19, 2022 are duplicated as the weekly vaccination pattern from December 1, 2022 (Sun) to February 1, 2023 (Wed). Since the daily number of the fourth dose vaccination is not yet available, we use the third dose vaccination records from December 1, 2021 (Wed) to August 10, 2022 (Wed) to surrogate the 4<sup>th</sup> dose vaccination data from May 25, 2022 (Wed) to February 1, 2023 (Wed), see the lower panel of Table S15 (<http://www.biosciencetrends.com/action/getSupplementalData.php?ID=134>).

At the end of November 2022, no further mutated virus has been discovered since the discovery of variant XBB on October 28, 2022. The current view is that BA.4 and BA.5 are still dominant variants in Japan. Recently, experts started to worry about variants BQ.1 and BQ1.1, descendants of BA.5, which are deemed to escape immunity and cause severe symptoms. Based on their judgements, variant BQ.1.1 is likely to become the next dominant variant (40).

### 3.1.2. Scenario creation

The statistics of Tokyo PCR testing performed in

November 2022 can be obtained from the Tokyo Metropolitan Government Website (1). For November 2022, the average number of PCR tests performed on a daily basis is 16,796. Multiplying by the scaling parameter and rounding it to a whole number, we obtain the daily PCR test number as 15 in our model. This number is defined as 'Normal' for estimating the future PCR tests statistics. In addition, we define the 'Active' state of PCR tests as doubling the testing number in the 'Normal' state.

We define 'Super active', 'Active' and 'Normal' scenarios (see Table S16, <http://www.biosciencetrends.com/action/getSupplementalData.php?ID=134>) to be situations where the number of travelers during the winter holiday season (2022.12.10 ~ 2023.01.10) is tripled, doubled and unchanged compared with that in November 2022. We assume that the number of daily PCR tests performed is doubled than that in November 2022, and the situation of daily in/outbound population is 'Super active' for Scenario I, 'Active' for Scenario II and 'Normal' for Scenario III during the winter holiday season (2022.12.10 ~ 2023.01.10). Additionally, we assume that the number of daily PCR tests is the same as that in November, and the daily in/outbound population is 'Super active' for scenario IV, 'Active' for scenario V and 'Normal' for scenario VI during the winter holiday season (2022.12.10 ~ 2023.01.10).

### 3.2. Results of forecasting

We repeated each simulation of the six scenarios 10 times and obtained the average results in Figure 3A. Overall, the forecast shows that the 8th wave shall peak around mid January and end around early March 2023.

From Figure 3A, we can see that the forecasted results from 2022.12.01 to 2023.03.01 are marked in red, light blue, green, deep blue, pink and brown lines, representing scenarios I, II, III, IV, V and VI respectively. It is clear that the number of daily PCR tests matters to the number of daily confirmed cases, the forecasted results of scenarios I, II and III apparently differentiate from scenarios IV, V and VI. Table S17 (<http://www.biosciencetrends.com/action/getSupplementalData.php?ID=134>) summarizes the key differences among the six scenarios, proving the significance of PCR testing to confirmed cases. While the effect of inbound and outbound tourists is, to some extent, subtle.

Figure 3B-G demonstrates the change in number of agents in E, I1 and I2 states in each of the six scenarios, with the number of E, I1 and I2 agents marked in purple, blue and red lines respectively. Table S18 (<http://www.biosciencetrends.com/action/getSupplementalData.php?ID=134>) summarizes the maximum number of unconfirmed (I1) and confirmed (I1 + I2) cases. The effect of inbound and outbound tourists is thus clear. Fewer the tourists, fewer unconfirmed, fewer total infections and earlier the maximum infection

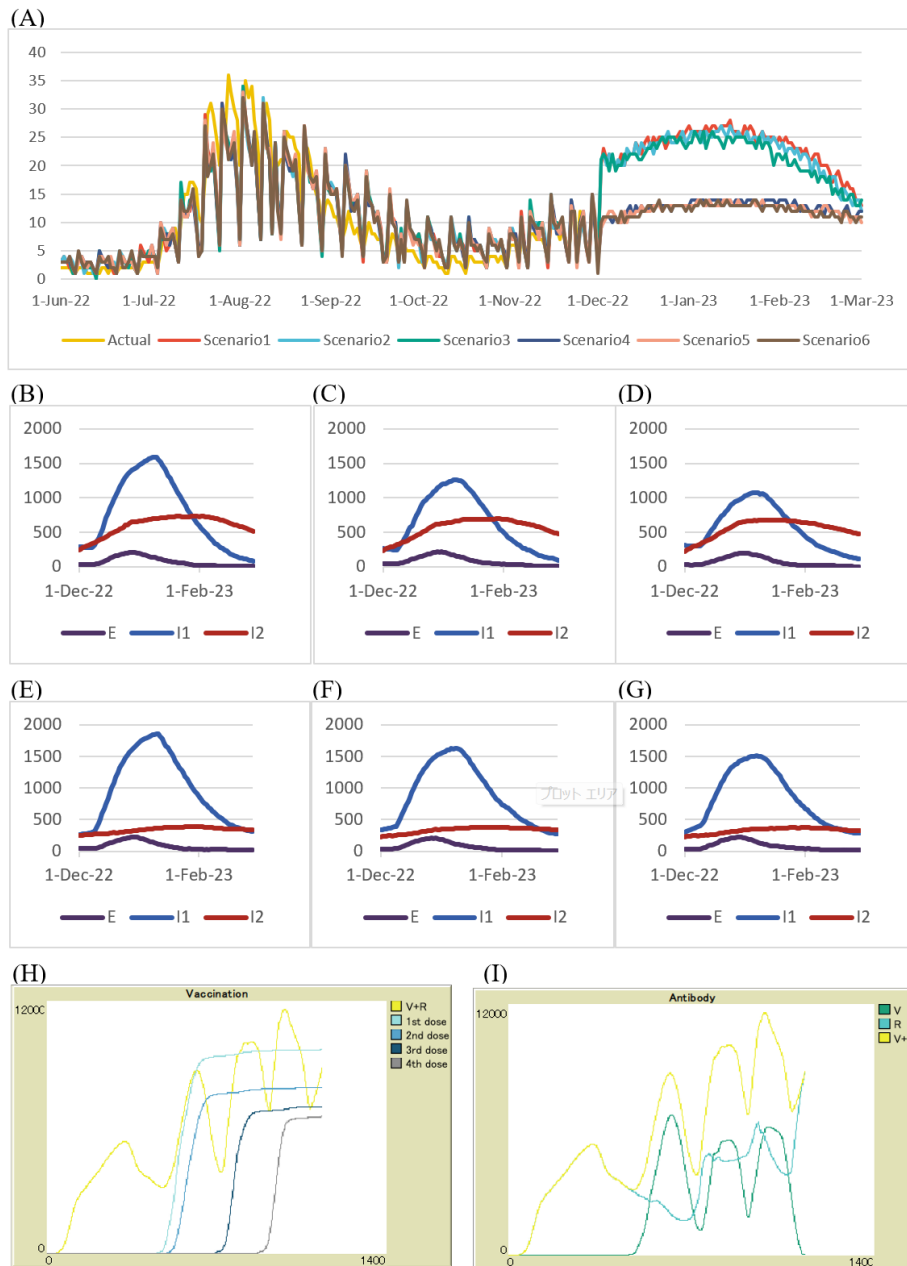


**Figure 3. Forecasted results based on 6 scenarios. (A),** Actual results post scaling, forecasted results of scenario I ~ VI, from June 1, 2022 to March 1, 2023. **(B) ~ (G),** The number of agents in E, I1 and I2 states for scenario I, II, III, IV, V and VI respectively. **(H) ~ (I),** In scenario IV, 4 doses of vaccination, the number of agents in V, R and V+R states from 2020.01.24 to 2023.03.01.

arrives. Figure 3H-I illustrates the simulation results of vaccination and antibody titer in scenario IV, with the number of V+R, V, R, 1st, 2nd, 3rd and 4th dose marked in yellow, dark green, light green, light blue, blue, dark blue, and gray lines respectively.

### 3.3. Findings

#### 3.3.1. Infection peak

1. Large scale PCR testing pushes back the peak of the infection, as can be inferred from Table S17 (<http://www.biosciencetrends.com/action/getSupplementalData.php?ID=134>), the infection peak of scenarios I~III is

around early to mid January, while that of scenarios IV~VI continues in late January.

2. An explosion in the number of travelers leads to more asymptomatic cases, confirmed cases and therefore postpones the arrival of the infection peak (see Table S17, <http://www.biosciencetrends.com/action/getSupplementalData.php?ID=134>).

#### 3.3.2. Optimal PCR tests

1. Faced with the currently low severe rate and death rate (severe rate = 0.01%, death rate = 0.001%), PCR tests would not make much difference to reduce overall infections, judging from the tiny difference of I1+I2

maximum. Specifically, between '1,930' in Scenario II and '1,989' in Scenario V, as well as '1,756' in Scenario III and '1,863' in Scenario VI (See Table S18, <http://www.biosciencetrends.com/action/getSupplementalData.php?ID=134>). Therefore, maintaining PCR tests to a low level helps to reduce both social cost and public anxiety.

2. As quoted from the Tokyo Metropolitan Government, the total number of hospital beds is 7,291 (1) to serve a total of 13,920,000 residents in Tokyo. and the total number of hospital beds targeting severe patients is 383. Based on the above simulation results, the total number of severe patients under infection peak is expected to be  $2,292 \div 0.0009 \times 0.01\% = 255 < 383$ . Therefore, we can conclude that, currently the medical resources are adequate.

3. However, if faced with a new variant in the future with high severe rate and death rate, PCR tests should be adjusted to a higher level to detect infection and start treatment early. Such a level of PCR tests should be compatible with available medical resources.

## 4. Discussion

### 4.1. Summary

This research demonstrates the importance of COVID-19 infection forecast in response to vaccine strategies, virus mutation, government policies and PCR testing. Specifically, this research approaches the problem using agent-based modeling and extended SEIR modeling methods. We justify the simplified social contact model as well as considering antibody titer declination in our research. After conducting simulation forecasts based on synthetic space and population, we conclude that the re-opening policy is subject to continuous monitoring. On one hand, the third-dose public vaccination rate is high; on the other, mutated variants like BQ.1 and BQ.1.1 are likely to become the next dominant variants due to significant evolving and immune escaping abilities (41). It is noted that the current trend of mutation is continuing, yet variants become more infective however less fatal. It is also pleasant to see the Tokyo Metropolitan Government has introduced and is encouraging a new round of vaccination against the BA. series. As is observed, the recovery of inbound foreign nations has started since October 11, 2022. It is suggested that continuous monitoring should be carried on with plans being made ahead for various scenarios.

### 4.2. Recommendations

Since Japan's opening-up policy (see Table S5, <http://www.biosciencetrends.com/action/getSupplementalData.php?ID=134>) cannot be reversed, the country should continue to monitor daily confirmed cases, detecting spreaders and closely monitoring possible mutation and new variants as well as severe rate and fatality rate (see

Table S2 and Table S4 (<http://www.biosciencetrends.com/action/getSupplementalData.php?ID=134>)). Although the trend of severe rate and fatality rate has been declining, there is no clear evidence to reject the claim that another troublesome variant with high fatality rate would not arrive in the near future.

In the meantime, the country is expected to improve hospital bed capacity. The current hospital bed occupancy rate has already reached 56.3% in Tokyo. Considering the possible mutated viruses brought by overseas travelers in December 2022 and January 2023, the existing medical resources are far from sufficient.

### 4.3. Future work

The battle against Coronavirus has lasted for three years. While we wait for the arrival of the final success in the near future, harder work should be carried out preventing possible resurgences and project corresponding reactions.

There are several flaws in the research. First is the moving pattern of agents. While we try to overcome the problem by putting forward the theory of large-scale flow dynamics, it is expected to be improved in the future. Second, natural birth and death rates have not been considered in the research, as well as family combination and separation (i.e marriage and divorce). In pursuit of model perfection, we shall make changes to population structure in the near future. Third, in this research we randomly select agents to conduct PCR tests, whereas in real world agents can freely choose whether to undertake PCR tests or not, based on their judgements to their own health. Lastly, as Dr. Israel once mentioned (32), the immune response elicited by vaccination or previous infection is a complex system, which is far from being entirely measured by the antibody titers. Although the clinical data of antibody titer can be obtained, we should apply and formulate such data to our studies with caution, in consideration of individual agents' heterogeneity of antibody titer level and decay rate.

Besides from the above, this study shall compare the simulated results with the public data of COVID-19 Infection in Tokyo, improve and try to forecast the March 2023 to June 2023 infection results, update possible new variants and immigration policies. Future study shall identify the influence of changes in vaccination strategies, immigration policies, virus mutation and PCR tests.

## Acknowledgements

This paper would not have been possible without the support from a number of important people. I'd like to thank M.D. Ariel Israel for his inspiring paper about IgG titer regression. Also, I'd like to extend my thanks to my friends and all members from the Simulation of Complex Systems (SCS) Laboratory.

**Funding:** This research received no specific grant from any funding agency in the public, commercial, or not-for-profit sectors.

**Conflict of Interest:** The authors have no conflicts of interest to disclose.

## References

1. Tokyo Metropolitan Government. Tokyo Metropolitan Government COVID-19 Information Website. <https://stopcovid19.metro.tokyo.lg.jp/en> (accessed January 19, 2023).
2. Chiba A. The effectiveness of mobility control, shortening of restaurants' opening hours, and working from home on control of COVID-19 spread in Japan. *Health Place*. 2021; 70:102622.
3. Yamauchi T, Takeuchi S, Uchida M, Saito M, Kokaze A. The association between the dynamics of COVID-19, related measures, and daytime population in Tokyo. *Sci Rep*. 2022; 12:1-12.
4. Murakami T, Sakuragi S, Deguchi H, Nakata M. Agent-based model using GPS analysis for infection spread and inhibition mechanism of SARS-CoV-2 in Tokyo. *Sci Rep*. 2022; 12:20896.
5. Yasuda H, Ito F, Hanaki K-i, Suzuki K. COVID-19 pandemic vaccination strategies of early 2021 based on behavioral differences between residents of Tokyo and Osaka, Japan. *Arch Public Health*. 2022; 80:1-12.
6. Larrauri B, Malbran A, Larrauri JA. Omicron and vaccines: An analysis on the decline in COVID-19 mortality. *medRxiv*. 2022. doi: 10.1101/2022.05.20.22275396.
7. Matsuyama K. Shionogi COVID-19 pill Xocova wins emergency approval in Japan | The Japan Times. <https://www.japantimes.co.jp/news/2022/11/22/national/science-health/shionogi-covid-xocova-approval/> (accessed January 19, 2023).
8. Urasaki Y. Japan to reopen to tour groups from 98 nations and regions | Nikkei Asia. <https://asia.nikkei.com/Business/Travel-Leisure/Japan-to-reopen-to-tour-groups-from-98-nations-and-regions> (accessed January 19, 2023).
9. Aoyama Y. First tour group from Hong Kong in 2 years lands at Narita Airport | The Asahi Shimbun. <https://www.asahi.com/ajw/articles/14652069> (accessed January 19, 2023).
10. Zhang Y. Australia's softball players are among the first Olympic athletes to arrive in Japan | The New York Times. <https://www.nytimes.com/2021/06/01/world/asia/australia-olympics-tokyo-japan-softball.html> (accessed January 19, 2023).
11. International Olympic Committee. Tokyo 2020 Olympic Village(s) Period of stay Guidelines for the NOCs. <https://stillmedab.olympic.org/media/Document%20Library/OlympicOrg/News/2020/12/Tokyo-2020-Olympic-Village-Guidelines-for-NOCs-in-relation-to-period-of-stay-eng.pdf> (accessed January 19, 2023).
12. McCurry J. 79,000 people flying in for Tokyo Olympics, Japanese media reports | The Guardian. <http://www.theguardian.com/sport/2021/may/20/organisers-of-tokyo-olympics-press-ahead-despite-covid-fears> (accessed January 19, 2023).
13. Tsukimori O. COVID tests still in short supply in Japan despite peak of sixth wave | The Japan Times. <https://www.japantimes.co.jp/news/2022/02/18/national/covid-tests-shortages/> (accessed January 19, 2023).
14. Ministry of Health, Labour and Welfare. COVID-19 tests. [https://www.mhlw.go.jp/stf/seisakunitsuite/bunya/0000121431\\_00182.html](https://www.mhlw.go.jp/stf/seisakunitsuite/bunya/0000121431_00182.html) (accessed January 19, 2023).
15. Tokyo Metropolitan Government. Test Kit Request Site for Close Contacts. <https://tokyo-testkit.metro.tokyo.lg.jp/closecontacts/form> (accessed January 19, 2023). (in Japanese)
16. Wilensky U. NetLogo. Northwestern University, Evanston, IL: Center for connected learning and computer-based modeling. 1999; <http://ccl.northwestern.edu/netlogo/> (accessed January 19, 2023).
17. Venkatramanan S, Lewis B, Chen J, Higdon D, Vullikanti A, Marathe M. Using data-driven agent-based models for forecasting emerging infectious diseases. *Epidemics*. 2018; 22:43-49.
18. Shamil M, Farheen F, Ibtehaz N, Khan IM, Rahman MS. An agent-based modeling of COVID-19: validation, analysis, and recommendations. *Cognit Comput*. 2021;1-12.
19. Li J, Giabbanelli P. Returning to a normal life via COVID-19 vaccines in the United States: a large-scale Agent-Based simulation study. *JMIR Med Inform*. 2021; 9:e27419.
20. Kerr CC, Stuart RM, Mistry D, Abeyururiya RG, Rosenfeld K, Hart GR, Núñez RC, Cohen JA, Selvaraj P, Hagedorn B. Covasim: an agent-based model of COVID-19 dynamics and interventions. *PLoS Comput Biol*. 2021; 17:e1009149.
21. Read JM, Bridgen JR, Cummings DA, Ho A, Jewell CP. Novel coronavirus 2019-nCoV (COVID-19): early estimation of epidemiological parameters and epidemic size estimates. *Philos Trans R Soc Lond B Biol Sci*. 2021; 376:20200265.
22. Yang HM, Junior LPL, Yang AC. Are the SIR and SEIR models suitable to estimate the basic reproduction number for the CoViD-19 epidemic? *MedRxiv*. 2020. doi: 10.1101/2020.10.11.20210831.
23. Li H, Leong FY, Xu G, Kang CW, Lim KH, Tan BH, Loo CM. Airborne dispersion of droplets during coughing: a physical model of viral transmission. *Sci Rep*. 2021; 11:1-10.
24. Live Japan. 6 Crazy Facts About Tokyo's Population (2021) - Inside the World's Top Megacity | LIVE JAPAN travel guide. [https://livejapan.com/en/in-tokyo/in-pref-tokyo/in-tokyo\\_suburbs/article-a0002533/](https://livejapan.com/en/in-tokyo/in-pref-tokyo/in-tokyo_suburbs/article-a0002533/) (accessed January 19, 2023).
25. Ministry of Internal Affairs & Communications. Japan Labor Force Participation Rate - December 2022 Data - 1953-2021 Historical | Trading Economics. <https://tradingeconomics.com/japan/labor-force-participation-rate> (accessed January 19, 2023).
26. MEXT (Japan). Japan: number of students at schools by prefecture 2021 | Statista. <https://www.statista.com/statistics/1192991/japan-number-students-schools-by-prefecture/> (accessed January 19, 2023).
27. Kadanoff LP, McNamara GR, Zanetti G. A Poiseuille viscometer for lattice gas automata. In: *Lattice Gas Methods for Partial Differential Equations*. Complex Syst. 1987; 1:791-803
28. Wolfram S, Gad-el-Hak M. A new kind of science. *Appl Mech Rev*. 2003; 56:B18-B19.
29. Ministry of Health, Labour and Welfare. COVID-19 Q&A. <https://www.mhlw.go.jp/stf/covid-19/qa.html> (accessed January 19, 2023).

30. Polack FP, Thomas SJ, Kitchin N, Absalon J, Gurtman A, Lockhart S, Perez JL, Marc GP, Moreira ED, Zerbini C. Safety and efficacy of the BNT162b2 mRNA Covid-19 vaccine. *N Engl J Med.* 2020; 383:2603-2615.
31. Yamaguchi T, Iwagami M, Ishiguro C, Fujii D, Yamamoto N, Narisawa M, Tsuboi T, Umeda H, Kinoshita N, Iguchi T. Safety monitoring of COVID-19 vaccines in Japan. *Lancet Reg Health West Pac.* 2022; 23:100442.
32. Israel A, Shenhar Y, Green I, Merzon E, Golan-Cohen A, Schäffer AA, Ruppin E, Vinker S, Magen E. Large-scale study of antibody titer decay following BNT162b2 mRNA vaccine or SARS-CoV-2 infection. *Vaccines.* 2022; 10:64.
33. Narasimhan M, Mahimainathan L, Araj E, Clark AE, Markantonis J, Green A, Xu J, SoRelle JA, Alexis C, Fankhauser K. Clinical evaluation of the Abbott Alinity SARS-CoV-2 spike-specific quantitative IgG and IgM assays among infected, recovered, and vaccinated groups. *J Clin Microbiol.* 2021; 59:e00388-00321.
34. Ebinger JE, Fert-Bober J, Printsev I, Wu M, Sun N, Probst JC, Frias EC, Stewart JL, Van Eyk JE, Braun JG. Antibody responses to the BNT162b2 mRNA vaccine in individuals previously infected with SARS-CoV-2. *Nat Med.* 2021; 27:981-984.
35. Regev-Yochay G, Gonen T, Gilboa M, Mandelboim M, Indenbaum V, Amit S, Meltzer L, Asraf K, Cohen C, Fluss R. Efficacy of a fourth dose of COVID-19 mRNA vaccine against omicron. *N Engl J Med.* 2022; 386:1377-1380.
36. Xu Q-Y, Xue J-H, Xiao Y, Jia Z-J, Wu M-J, Liu Y-Y, Li W-L, Liang X-M, Yang T-C. Response and duration of serum anti-SARS-CoV-2 antibodies after inactivated vaccination within 160 days. *Front Immunol.* 2021; 12.
37. Karako K, Song P, Chen Y, Tang W, Kokudo N. Overview of the characteristics of and responses to the three waves of COVID-19 in Japan during 2020-2021. *Biosci Trends.* 2021; 15:1-8.
38. Patil I. Visualizations with statistical details: The 'ggstatsplot' approach. *J. Open Source Softw.* 2021; 6:3167.
39. Sheward DJ, Kim C, Fischbach J, Sato K, Muschiol S, Ehling RA, Björkström NK, Hedestam GBK, Reddy ST, Albert J. Omicron sublineage BA. 2.75. 2 exhibits extensive escape from neutralising antibodies. *Lancet Infect Dis.* 2022; 22:1538-1540.
40. Edamatsu Y. Experts warn BQ.1 becoming dominant virus strain in Japan | The Asahi Shimbun. <https://www.asahi.com/ajw/articles/14787896> (accessd January 19, 2023).
41. Ito J, Suzuki R, Uriu K, Itakura Y, Zahradnik J, Deguchi S, Wang L, Lytras S, Tamura T, Kida I. Convergent evolution of the SARS-CoV-2 Omicron subvariants leading to the emergence of BQ. 1.1 variant. *bioRxiv.* 2022. doi: 10.1101/2022.12.05.519085.
42. Novel Coronavirus Domestic Infection Situation | Toyo keizai Online. <https://toyokeizai.net/sp/visual/tko/covid19/> (accessd January 19, 2023). (in Japanese)
43. Higashide M. Ratio of severely ill patients (to number of patients receiving medical treatment). <https://uub.jp/cvd/> (accessd January 19, 2023). (in Japanese)
44. Fujii D, Nakata T. COVID-19 and economic activity in Japan. <https://covid19outputjapan.github.io/JP/> (accessd January 19, 2023). (in Japanese)

Received January 15, 2023; Revised February 8, 2023; Accepted February 9, 2023.

*\*Address correspondence to:*

Yu Chen, SCS Laboratory, Room 216, Environment Building, The University of Tokyo Kashiwa Campus, Kashiwanoha 5-1-5, Kashiwa, Chiba 277-8563, Japan.  
E-mail: chen@edu.k.u-tokyo.ac.jp

Released online in J-STAGE as advance publication February 11, 2023.